Progress In Electromagnetics Research M, Vol. 99, 129–138, 2021

Scattering from a Rectangular Dielectric Cylinder by Mode Matching Technique

Muhammad Akbar[1, *] and Saeed Ahmed[2]

Abstract—The propagated fields within and radiated fields outside a rectangular dielectric cylinder are represented as guided and radiation modes respectively. These fields of the cylinder are related with incident, backward scattered fields at $x = 0$ and transmitted fields at $x = a$ by Mode Matching technique. The expressions for guided and radiation mode amplitudes are derived by applying the orthogonal property of the modes. The unknown functions (mode amplitudes) in each of these equations that are defining discrete functions of the guided modes field and angular spectrum for the radiation field are determined numerically. The powers due to discrete guided modes (even and odd) are calculated. The integrals related with the backward and forward scattered fields and the powers associated with them are approximately evaluated by the method of steepest descents.

1. INTRODUCTION

The cylinders represent one of the most important classes of geometrical object used for important civil and military wide applications. The numerical simulation of the scattering from cylinders has a long history in computational electromagnetics. Froese and Wait [1] investigated the diffracted field due to dielectric cylinder whose parameters correspond to the experimental conditions. Similar diffraction has been considered by Wait [2] in which he considered the interaction of electromagnetic waves with plasma cylinder which is placed in the free space. Very few researchers have considered a dielectrics cylinder with rectangular geometry [3, 4]. In this paper, we will consider the fields due to a rectangular dielectric cylinder as guided and radiation modes and relate these fields with the incident and scattered fields by applying the Mode Matching technique which is frequently used in electromagnetics for complex geometries [5]. The resulting expressions are simplified by the orthogonal properties of the modes and will derive the expressions of their mode amplitudes (guided and radiations) not only in the forward direction but also in the backward direction. The backward and forward scattering coefficients $R(k_{1y})$ and $T(k_{1y})$ are determined numerically. Moreover, the power propagated (forward and backward) within dielectric cylinder is determined numerically. The back and forward scattered fields and power in the free space are approximated asymptotically.

2. MATHEMATICAL FORMULATION

The electromagnetic propagation and scattering are considered in which a plane wave (E-polarized) is incident at angle $\theta_i = \frac{\pi}{4}$ with the rectangular dielectric cylinder of length a and width $2b$ as shown in Fig. 1. The dimension of the dielectric cylinder along z-axis is taken to be infinite. The energy is bounded within the cylinder partially due to the bouncing of the waves not only in upward-downward

Received 11 July 2020, Accepted 20 November 2020, Scheduled 7 December 2020

* Corresponding author: Muhammad Akbar (akbar5508126@yahoo.com).

[1] Department of Electronics, Quaid-i-Azam University, Islamabad, Pakistan. [2] Department of Earth Sciences, Quaid-i-Azam University, Islamabad, Pakistan.

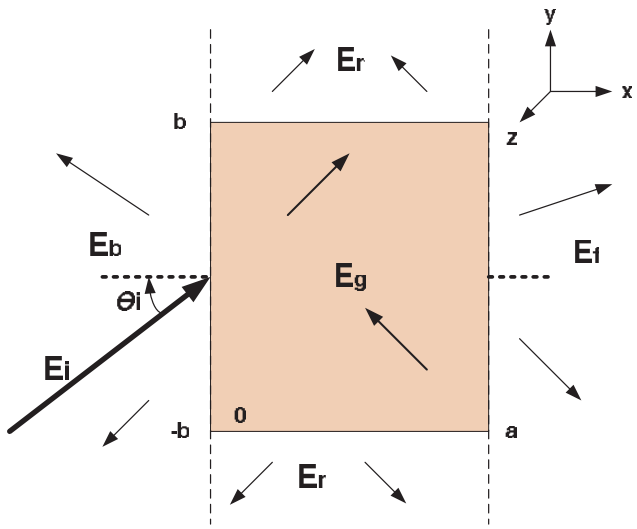

Figure 1. Scattering due to dielectric cylinder.

but also in forward-backward directions. The fields carrying this energy are in the form of even and odd guided modes in forward-backward direction. Due to the presence of discontinuity, the energy is also radiated in the free space as radiation modes [9]. These guided modes (forward and backward) and the radiation modes of the dielectric cylinder are represented as follows.

3. GUIDED AND RADIATION MODES

Here various notations used for the electric field representations in the following evaluations should be taken as: an 'eg' in the subscript stands for even guided with an 'og' in the subscript for odd guided mode. Similarly a '+' in the superscript stands for positive (+) x-axis while a '−' in the superscript stands for negative (−) x-axis. The expanded form of the field expressions for guided and radiation modes in each region are as follows.

3.1. Even Guided Modes

$$E_{eg}^{(n)}(x,y) = \begin{cases} \left\{[A_n^+ e^{ik_{xn}x}] + [A_n^- e^{-ik_{xn}x}]\right\} k_{2n} e^{-k_{1n}(y-b)} & 0 < x < a, \quad y > b\,; \\ \left\{[A_n^+ e^{ik_{xn}x}] + [A_n^- e^{-ik_{xn}x}]\right\} [(k_{2n} + ik_{1n})\cos(k_{2n}y)] & 0 < x < a, \quad |y| < b\,; \\ \left\{[A_n^+ e^{ik_{xn}x}] + [A_n^- e^{-ik_{xn}x}]\right\} k_{2n} e^{k_{1n}(y+b)} & 0 < x < a, \quad y < -b; \end{cases}$$

A linear combination of all such solutions for even guided modes is written as,

$$E_{eg}^{(n)}(x,y) = \sum_{n=1}^{N} \left\{[A_n^+ e^{ik_{xn}x}] + [A_n^- e^{-ik_{xn}x}]\right\} F_{eg}^{(n)}(y) \tag{1}$$

3.2. Odd Guided Modes

Similarly the field expression for odd guided mode due to dielectric cylinder, which includes all the regions, is,

$$E_{og}^{(p)}(x,y) = \begin{cases} -\left\{[A_p^+ e^{ik_{xp}x}] + [A_p^- e^{-ik_{xp}x}]\right\} k_{2p} e^{-k_{1p}(y-b)} & 0 < x < a, \quad y > b; \\ i\left\{[A_p^+ e^{ik_{xp}x} + A_p^- e^{-ik_{xp}x}\right\} [(k_{2p} + ik_{1p})\sin(k_{2p}y)] & 0 < x < a, \quad |y| < b; \\ \left\{[A_p^+ e^{ik_{xp}x}] + [A_p^- e^{-ik_{xp}x}]\right\} k_{2p} e^{k_{1p}(y+b)} & 0 < x < a, \quad y < -b; \end{cases}$$

Similarly, the general field expression of the all odd guided modes for a dielectric cylinder can be represented as the linear combination of all the modes

$$E_{og}^{(p)}(x,y) = \sum_{p=1}^{P} \left\{ [A_p^+ e^{ik_{xp}x}] + [A_p^- e^{-ik_{xp}x}] \right\} F_{og}^{(p)}(y) \tag{2}$$

The solution of Helmholtz's equation leads to plane waves. After applying the boundary conditions at $-b$ and b, a set of four equations is derived. For their non-trivial solution, two transcendental equations for even and odd guided modes were derived. The roots of these equations which are the eigenvalues of these eigenvalue equation were determined numerically [6].

3.3. Radiation Modes

Radiation modes of the dielectric cylinder carry energy away into the free space. These modes carry energy not only in the forward direction but also in the backward direction. After putting the values of the coefficients the field expression of radiation modes is,

$$E_r(x,y) = \begin{cases} \left\{A^+ e^{ik_x x} + A^- e^{-ik_x x}\right\} \left[T e^{ik_{1y}(y-b)}\right] & 0 < x < a, \quad y > b; \\ \left\{A^+ e^{ik_x x} + A^- e^{-ik_x x}\right\} \left[B e^{ik_{2y}y} + C e^{-ik_{2y}y}\right] & 0 < x < a, \quad |y| < b; \\ \left\{A^+ e^{ik_x x} + A^- e^{-ik_x x}\right\} \left[e^{ik_{1y}(y+b)} + R e^{-ik_{1y}(y+b)}\right] & 0 < x < a, \quad y < -b; \end{cases}$$

where,

$$R = \frac{-\left[1 - \left(\frac{k_{1y}}{k_{2y}}\right)^2\right] \sin(2k_{2y}b)}{\left[1 + \left(\frac{k_{1y}}{k_{2y}}\right)^2\right] \sin(2k_{2y}b) + 2i\left(\frac{k_{1y}}{k_{2y}}\right) \cos(2k_{2y}b)} \tag{3}$$

Similarly, the expressions of T, B, and C can be derived as,

$$T = \frac{2i\left(\frac{k_{1y}}{k_{2y}}\right)}{\left[1 + \left(\frac{k_{1y}}{k_{2y}}\right)^2\right] \sin(2k_{2y}b) + 2i\left(\frac{k_{1y}}{k_{2y}}\right) \cos(2k_{2y}b)} \tag{4}$$

$$B = \frac{1}{2}\left(1 + \frac{k_{1y}}{k_{2y}}\right) T e^{-ik_{2y}b} \tag{5}$$

And

$$C = \frac{1}{2}\left(1 - \frac{k_{1y}}{k_{2y}}\right) T e^{ik_{2y}b} \tag{6}$$

A linear combination of all such solutions for radiation modes for all values of k_{1y} will also represent a solution to the Helmholtz's equation. This statement can be mathematically written as,

$$E_r(x,y) = \int_0^\infty \left\{ A^+(k_{1y}) e^{ik_x x} + A^-(k_{1y}) e^{-ik_x x} \right\} F_r(k_{1y}, y) dk_{1y} \tag{7}$$

4. MODE AMPLITUDES AND FUNCTIONAL EQUATION

The fields are continuous across the interfaces at $x = 0$ and $x = a$. The coupling of incident, back scattering, and forward scattering fields with the modal fields of the cylinder is carried out by Mode Matching [7, 8]. Modal fields due to cylinder are represented by guided as well as radiation modes and are shown in Equations (1), (2), and (7). The back scattering and forward scattering fields are plane wave spectrums. As a result, four equations of continuity are derived. The orthogonal property of the modes is utilized to simplify the field expression and to derive the expression of mode amplitudes of the guided as well as radiation modes. The mode amplitudes of guided modes (even and odd) propagating in forward and backward directions are as follows.

4.1. Mode Amplitudes for Guided Modes

$$A_n^+ = \int_{-\infty}^{\infty} R\left(k_{1y}\right) \left\{ \frac{\left[\sqrt{k_2^2 - k_{2n}^2} - \sqrt{k_1^2 - k_{1y}^2}\right] \left[F_e^{(n)}\left(k_{1y}\right)\right]}{2F_e^{(n)}\sqrt{k_2^2 - k_{2n}^2}} \right\} dk_{1y} + \left\{ \frac{\left[k_1' + \sqrt{k_2^2 - k_{2n}^2}\right] \left[F_{1e}^{(n)}\right]}{2F_e^{(n)}\sqrt{k_2^2 - k_{2n}^2}} \right\}. \quad (8)$$

And,

$$A_n^- = \int_{-\infty}^{\infty} R(k_{1y}) \left\{ \frac{\left[\sqrt{k_2^2 - k_{2n}^2} + \sqrt{k_1^2 - k_{1y}^2}\right] \left[F_e^{(n)}(k_{1y})\right]}{2F_e^{(n)}\sqrt{k_2^2 - k_{2n}^2}} \right\} dk_{1y} - \left\{ \frac{\left[k_1' - \sqrt{k_2^2 - k_{2n}^2}\right] \left[F_{1e}^{(n)}\right]}{2F_e^{(n)}\sqrt{k_2^2 - k_{2n}^2}} \right\}. \quad (9)$$

Similarly, the mode amplitude for odd guided modes can be derived,

$$A_p^+ = \int_{-\infty}^{\infty} R(k_{1y}) \left\{ \frac{\left[\sqrt{k_2^2 - k_{2p}^2} - \sqrt{k_1^2 - k_{1y}^2}\right] \left[F_o^{(p)}(k_{1y})\right]}{2F_o e^{(p)}\sqrt{k_2^2 - k_{2p}^2}} \right\} dk_{1y} + \left\{ \frac{\left[k_1' + \sqrt{k_2^2 - k_{2p}^2}\right] \left[F_{1o}^{(p)}\right]}{2F_o^{(p)}\sqrt{k_2^2 - k_{2p}^2}} \right\}. \quad (10)$$

And,

$$A_p^- = \int_{-\infty}^{\infty} R(k_{1y}) \left\{ \frac{\left[\sqrt{k_2^2 - k_{2p}^2} + \sqrt{k_1^2 - k_{1y}^2}\right] \left[F_o^{(p)}(k_{1y})\right]}{2F_o^{(p)}\sqrt{k_2^2 - k_{2p}^2}} \right\} dk_{1y} - \left\{ \frac{\left[k_1' - \sqrt{k_2^2 - k_{2p}^2}\right] \left[F_{1o}^{(p)}\right]}{2F_o^{(p)}\sqrt{k_2^2 - k_{2p}^2}} \right\} \quad (11)$$

where,

$$\begin{aligned}
F_e^{(n)} &= 2\frac{k_{2n}}{k_{1n}} + 2bF_n^* \frac{\sin\left(k_{2n}b\right)}{\left(k_{2n}b\right)} \\
F_e^{(n)}\left(k_{1y}\right) &= i\left\{ \frac{k_{2n}e^{ik_{1y}b}}{\left(k_{1y} + ik_{1n}\right)} - \frac{k_{2n}e^{-ik_{1y}b}}{\left(k_{1y} - ik_{1n}\right)} \right\} + F_n^* \left\{ \frac{\sin\left(k_{1y} + k_{2n}\right)b}{\left(k_{1y} + k_{2n}\right)} + \frac{\sin\left(k_{1y} - k_{2n}\right)b}{\left(k_{1y} - k_{2n}\right)} \right\} \\
F_{1e}^{(n)} &= \left\{ \frac{k_{2n}e^{-ik_1'b}}{\left(k_{1n} + ik_1'\right)} + \frac{k_{2n}e^{ik_1'b}}{\left(k_{1n} - ik_1'\right)} \right\} + F_n^* \left\{ \frac{\sin\left(k_{2n} + k_1'\right)b}{\left(k_{2n} + k_1'\right)} + \frac{\sin\left(k_{2n} - k_1'\right)b}{\left(k_{2n} - k_1'\right)} \right\} \\
F_o^{(p)}\left(k_{1y}\right) &= -i\left\{ \frac{k_{2p}e^{ik_{1y}b}}{\left(k_{1y} + ik_{1p}\right)} + \frac{k_{2p}e^{-ik_{1y}b}}{\left(k_{1y} - ik_{1p}\right)} \right\} - F_p^* \left\{ \frac{\sin\left(k_{1y} + k_{2p}\right)b}{\left(k_{1y} + k_{2p}\right)} - \frac{\sin\left(k_{1y} - k_{2p}\right)b}{\left(k_{1y} - k_{2p}\right)} \right\}
\end{aligned}$$

And,

$$\begin{aligned}
F_{1o}^{(p)} &= \left\{ \frac{k_{2p}e^{-ik_1'b}}{\left(k_{1p} + ik_1'\right)} - \frac{k_{2p}e^{ik_1'b}}{\left(k_{1p} - ik_1'\right)} \right\} - F_p^* \left\{ \frac{\sin\left(k_{2p} + k_1'\right)b}{\left(k_{2p} + k_1'\right)} - \frac{\sin\left(k_{2p} - k_1'\right)b}{\left(k_{2p} - k_1'\right)} \right\} \\
F_o^{(p)} &= \left\{ \frac{k_{2p}^2}{k_{1p}} + \left(k_{2p}^2 + k_{1p}^2\right)\left[\frac{\sin\left(2k_{2p}b\right)}{2k_{2p}} - b\right] \right\}
\end{aligned}$$

where,

$$k_1' = k_1 \sin\frac{\pi}{4}.$$

These guided mode amplitudes expressed by Eq. (8) through Eq. (11) can only be determined if $R(k_{1y})$ in the given equations are known. Hence, a functional equation is to be derived which is to be solved numerically to determine the reflection coefficients $R(k_{1y})$.

4.2. Derivation of Functional Equation

In the case of rectangular dielectric cylinder, we have four field equations by applying the boundary conditions at $x = 0$ and $x = a$. After applying the orthogonal properties of the modes, these equations are simplified having only four unknowns $A^+(k_{1y})$, $A^-(k_{1y})$, $R(k_{1y})$, and $T(k_{1y})$. Solving these equations

simultaneously $A^+(k_{1y})$, $A^-(k_{1y})$ can be eliminated. As a result, the following functional equation is derived which couples the backward scattering coefficients $R(k_{1y})$ and the forward scattering coefficient $T(k_{1y})$.

$$\int_{-\infty}^{\infty} R\left(k_{1y}\right)\left\{\left(k'_x+k_x\right)\left[F\left(k_{1y},k'_{1y}\right)\right]\right\}dk_{1y}$$
$$+e^{ik'_x a}\int_{-\infty}^{\infty} T\left(k_{1y}\right)\left\{\left(k_x-k'_x\right)\left[F\left(k_{1y},k'_{1y}\right)\right]\right\}dk_{1y}\left\{k'_1-k'_x\right\}\left[F(k'_{1y}\right] \tag{12}$$

$$\begin{aligned} F\left(k'_{1y},k_{1y}\right) &= \pi\left\{\left[e^{-ik_{1y}b}+T'e^{ik_{1y}b}\right]\delta\left(k_{1y}-k'_{1y}\right)+\left[R'e^{-ik_{1y}b}\delta\left(k_{1y}+k'_{1y}\right)\right]\right\} \\ &\quad +i\left\{\frac{-e^{-ik_{1y}b}}{\left(k_{1y}-k'_{1y}\right)}+\frac{T'e^{ik_{1y}b}}{\left(k_{1y}-k'_{1y}\right)}-\frac{R'e^{-ik_{1y}b}}{\left(k_{1y}+k'_{1y}\right)}\right\} \\ &\quad +2\left\{B'\frac{\sin\left(k_{1y}-k'_{2y}\right)b}{\left(k_{1y}-k'_{2y}\right)}+C'\frac{\sin\left(k_{1y}+k'_{2y}\right)b}{\left(k_{1y}+k'_{2y}\right)}\right\} \\ F\left(k'_{1y}\right) &= \frac{i}{k'_{1y}}\left(1-R'-T'\right)+2b\left(B'+C'\right)\frac{\sin\left(k'_{2y}b\right)}{\left(k'_{2y}b\right)} \end{aligned} \tag{13}$$

This is the general functional Equation (12) which relates the backward and forward parts of the scattered field of cylinder. This equation is solved numerically by known techniques (Method of Moments) to determine $R(k_{1y})$ and $T(k_{1y})$ [10]. Once the free space mode amplitudes are determined, all the amplitudes of even and odd guided modes shown in above equations can be determined.

5. THE POWER WITHIN DIELECTRIC CYLINDER

The guided waves in the dielectric cylinder are not only moving in forward direction but also in the backward direction after bouncing back from the interface at $x = a$. As a result, a part the field and power is trapped within the body of dielectric medium. This field is in the form of even and odd guide modes moving along forward and backward directions. The mode amplitudes of these guided modes are A_n^+, A_n^-, A_p^+, and A_p^-. These mode amplitudes are already determined by using relationsin Eqs. (8) through (11). Here the field and power expressions for even and odd guided modes are derived and determined.

The field expression for the nth even guided mode is,

$$E_e^{(+n)}(x,y) = A_n^+\left[F^{(n)}\cos(k_{2n}y)\right]e^{ik_{xn}x} \quad 0<x<a, \quad |y|<b \tag{14}$$

The power carried by this nth mode is

$$P_n^+ = \int \vec{S^+}\cdot e_x dx$$

where S^+ is a pointing vector.

$$P_n^+ = A_n^+ A_n^{+*}\left[\frac{\sqrt{\epsilon_r}}{2\eta}\left(k_{2n}^2+k_{1n}^2\right)\right]\int_{-b}^{b}\cos^2\left(k_{2n}y\right)dy$$

The equation can be solved as,

$$P_n^+ = \left|A_n^+\right|^2\left\{2b\frac{\sqrt{\epsilon_r}}{\eta}\left(k_{2n}^2+k_{1n}^2\right)\right\} \tag{15}$$

Similarly, the power propagated in the backward direction due to even guided modes is

$$P_n^- = \left|A_n^-\right|^2\left\{2b\frac{\sqrt{\epsilon_r}}{\eta}\left(k_{2n}^2+k_{1n}^2\right)\right\} \tag{16}$$

The expression of electric field which is confined within the slab due to the pth odd mode propagating in the forward direction is,

$$E_o^{(+p)}(x,y) = A_p^+ F^{(p)} \sin(k_{2p}y) e^{ik_{xp}x}, \quad 0 < x < a, \quad |y| < b \tag{17}$$

Now its expression of power can be written as,

$$P_p^+ = |A_p^+|^2 \left\{ 2b \frac{\sqrt{\epsilon_r}}{\eta} \left(k_{2p}^2 + k_{1p}^2 \right) \right\} \tag{18}$$

Similarly, the power propagated in the backward direction due to the pth odd guided modes is

$$P_p^- = \left|A_p^-\right|^2 \left\{ 2b \frac{\sqrt{\epsilon_r}}{\eta} \left(k_{2p}^2 + k_{1p}^2 \right) \right\} \tag{19}$$

The guided power carried by each of these modes and its variation with respect cylinder width 'b' are shown in the following Table 1.

6. THE BACKWARD AND FORWARD SCATTERING POWER OF DIELECTRIC CYLINDER

The functional Equation (12) is solved numerically to determine $R(k_{1y})$ and $T(k_{1y})$ for the backward and forward scattered fields, respectively. Now the backward and forward scattered fields and their respective powers due to dielectric cylinder in their corresponding regions of space are to be determined. To achieve this objective, the integral equations for the scattered fields are to be solved asymptotically [11].

The integral representation of backward scattered field E_b in the region of $x < 0$ and $\forall y$ is,

$$E_b(x,y) = \int_{-\infty}^{\infty} R(k_{1y}) e^{-ik_x x + ik_{1y} y} dk_{1y} \tag{20}$$

Transformation from k_{1y} to ϕ plane will be carried out to facilitate the evaluation of the integral according to

$$k_{1y} = k_1 \sin\phi, \quad k_x = k_1 \cos\phi$$

Similarly, the cartesian coordinates x and y are transformed to polar coordinates r and θ using,

$$x = -r\cos\theta, \quad y = r\sin\theta.$$

The asymptotic solution of this equation is,

$$E_b(r,\theta) = R(\theta)\, F_b(\theta) \frac{e^{ik_1 r}}{\sqrt{k_1 r}} \quad \frac{-\pi}{2} < \theta < \frac{\pi}{2} \tag{21}$$

where,

$$F_b(\theta) = \left[\sqrt{2\pi}\, \cos\theta\, e^{i\pi/4} \right]$$

Hence, the backward scattered power of the cylinder is

$$P_b(\theta) = |R(\theta|^2\, |F_b(\theta|^2 \quad \frac{-\pi}{2} < \theta < \frac{\pi}{2} \tag{22}$$

Numerical investigation of the backward scattered power P_b versus observation angle θ is presented which demonstrates that the scattered power is significantly influenced by width 'b' of the cylinder.

Similarly, the integral representation of forward scattered field E_f in the region of $x > a$ and $\forall y$ is,

$$E_f(x,y) = \int_{-\infty}^{\infty} T(k_{1y}) e^{ik_x x + ik_{1y} y}\, dk_{1y} \tag{23}$$

$T(k_{1y})$ is the forward scattering coefficients whose values are already determined numerically. The asymptotic solution of this equation results into

$$E_f(r,\theta) = T(\theta)\, F_f(\theta) \frac{e^{ik_1 r}}{\sqrt{k_1 r}} \quad \frac{-\pi}{2} < \theta < \frac{\pi}{2} \tag{24}$$

Table 1. Power carried by the guided modes for different values of cylinder width b, where incident angles $\theta_i = \frac{\pi}{4}$, and $\epsilon_r = 3.12$.

$b = 0.05\lambda$	Even	Forward	Eigenvalues	1.33	0	0
			Modal Power	−40.3	0	0
			Prop Angles	49	0	0
		Backward	Modal Power	−55.7	0	0
			Prop Angles	131	0	0
	Odd	Forward	Eigenvalues	0	0	0
			Modal Power	0	0	0
			Prop Angles	0	0	0
		Backward	Modal Power	0	0	0
			Prop Angles	0	0	0
$b = 0.12\lambda$	Even	Forward	Eigenvalues	1.035	0	0
			Modal Power	−34.9	0	0
			Prop Angles	36	0	0
		Backward	Modal Power	−50.2	0	0
			Prop Angles	144	0	0
	Odd	Forward	Eigenvalues	−0.985	−0.981	0
			Modal Power	−35.2	−35	0
			Prop Angles	−44.0	34	0
		Backward	Modal Power	−51.0	−50.5	0
			Prop Angles	−146	146	0
$b = 0.52\lambda$	Even	Forward	Eigenvalues	−1.16	−0.61	0.39
			Modal Power	−33.8	−37.0	−37.7
			Prop Angles	−41.0	−20.0	13
		Backward	Modal Power	−48.9	−52.7	−52.5
			Prop Angles	−139	−160	167
	Odd	Forward	Eigenvalues	−0.78	0.78	0
			Modal Power	−19.5	−19.5	0
			Prop Angles	−26.0	26.0	0
		Backward	Modal Power	−35.0	−34.8	0
			Prop Angles	−153	153	0

where,

$$F_f(\theta) = \left[\sqrt{2\pi}\,\cos\theta\, e^{i\pi/4}\right]$$
$$P_f(\theta) = |T(\theta|^2|F_f(\theta|^2 \quad \frac{-\pi}{2} < \theta < \frac{\pi}{2} \tag{25}$$

Here the forward scattered power P_f versus observation θ is presented which demonstrate that the forward scattered power is also significantly influenced by width 'b' of the cylinder.

7. NUMERICAL RESULTS AND DISCUSSIONS

Here the physical interpretation of the numerical results is presented. According to the theory, a dielectric cylinder having rectangular dimensions is excited by a plane wave incident obliquely. As a result, all guided as well as radiation modes are excited to satisfy the boundary conditions at the

discontinuities. This dielectric cylinder can possess finite number of guided modes in addition to a continuum of unguided radiation modes. The guided modes (even and odd) carry power essentially within the dielectric cylinder not only in forward direction but also in backward direction. These guided modes are eigen-modes having eigenvalues. The number of eigenvalues and their corresponding eigen-modes depends upon the electrical length of the cylinder which is a measure of relative permittivity ϵ_r of the medium of dielectric cylinder and its width of b. The expressions for the determination of eigenvalues of the given structure are derived but not reported here. As we increase the electrical length of structure by either increasing the relative permittivity ϵ_r of the medium of dielectric cylinder or its width b, there is an increase of the number of guided modes. Here we can see from the table that for $\epsilon_r = 3.12$ and $b = 0.05\lambda$ only one eigenvalue can exist having one even guided mode which is propagating in forward direction at a particular propagation angle with horizontal axis and bounced back with less power after loosing much power at the boundary $x = a$ along another propagation angle. For the cylinder width $b = 0.12\lambda$ having constant $\epsilon_r = 3.12$, three eigenvalues (one even and two odd) are possible, and hence one even and two odd modes are capable to propagate at particular propagation angles in the forward direction. These will return back after loosing the considerable amount of power at specific propagation angles. For a thicker cylinder of thickness $b = 0.52\lambda$, three even and two odd modes can propagate and bounce back after loosing power at the cylinder boundary.

Each column of the table describes the eigenvalue (dimensionless) of the particular eigen mode, the power (dB) carried by this mode, and the propagation angle (deg) of this mode and bounce back after loosing power at the cylinder boundary ($x = a$) at a particular propagation angle.

Although it is very difficult to accurately find the power radiated by the waves around the dielectric cylinder because of the bounded field due to forward and backward bouncing of the guided modes and spill over from its surfaces and diffracted from its edges as radiation modes, the scattering around the cylinder can be estimated by analytico-numerical approach. The scattering coefficients for forward and backward directions $R(k_{1y})$ and $T(k_{1y})$ are calculated numerically. The forward (A^+) and backward (A^-) scattering coefficients in the regions $(0 < x < a, y < -b)$ and $(0 < x < a, y > b)$ are lengthy, complicated, and are calculated but not reported here. The detail will be provided in followup papers.

Here we have considered only the back and forward scattered parts of the power. For the better understanding of the scattering in forward and backward directions, it is advisable to see the variation of spatial domain of the problem with reference to observation angle. For the backward scattering $\frac{-\pi}{2} < \theta < 0$ means the third quadrant while $0 < \theta < \frac{\pi}{2}$ means the second quadrant. Similarly for forward scattering, $\frac{-\pi}{2} < \theta < 0$ means the fourth quadrant while $0 < \theta < \frac{\pi}{2}$ means the first quadrant.

Comparison of the two plots shows that two peaks are observed in backward scattering power and two peaks are in forward scattering power. These peaks are due to the diffraction from the four wedges of the cylinder. Comparatively, more power is scattered in the forward direction than the backward direction. Moreover, it is observed that more power is scattered at angle of $\theta = \frac{\pi}{4}$ in the first quadrant. This is because at this angle the incident field and diffracted fields reinforce each other. The backward part of the power is essentially coupled to the radiation modes of the free space. If the spilled over part of the power is ignored, then the total field in this region consists of reflected and diffracted components. The reflected field is the field reflected from the plane surface of the cylinder having width $2b$ with edge ignored, and the diffracted field is due to two edges of the cylinder. Now the variation of reflected power with respect to width of the cylinder is considered for a given incidence angle ($\theta_i = \frac{\pi}{4}$) in Fig. 2. It is observed that the general pattern of reflected power observed is same for all widths of the cylinder. A few important features are observed in this plot. First, the reflected power is relatively less for smaller width, and there is an increase of power when the cylinder width is increased. This is because for a smaller width, the face area of the cylinder on which the incident wave impinges is small, so less power is scattered in backward direction. Second, the number of peaks in the reflected pattern is small for smaller cylinder width than the case when the width of the cylinder is large. This is because the number of guided modes increases with cylinder width. It is also observed that much backward scattered power is along $\theta_r = \frac{\pi}{4}$. This is because at this angle reflected and diffracted parts of the field superpose each other. As a result, maximum power is scattered in this direction.

The forward scattering field in the region $x > a$ is composed of an incident plane wave, transmitted from the body of the dielectric cylinder plus diffracted fields which emanate from the two edges of the cylinder. The incident wave shows the geometrical optics solution while the field discontinuity at $x = a$

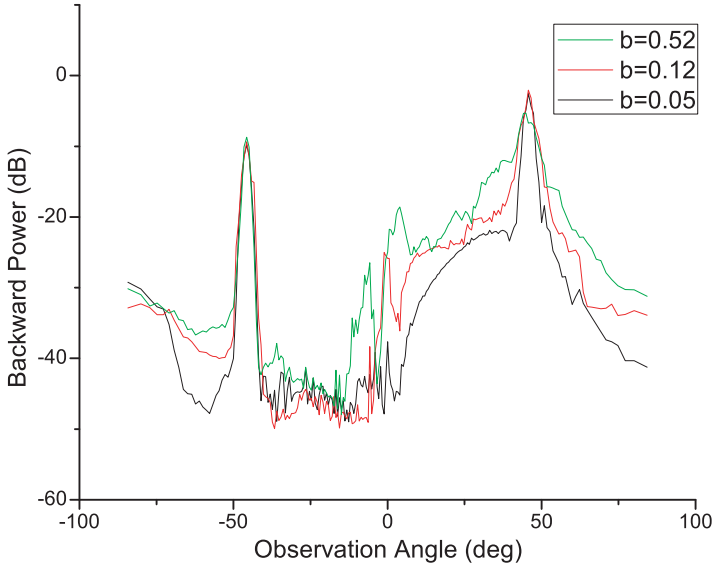

Figure 2. Backward scattered power of a dielectric cylinder for different values of its 'b', where $\epsilon_r = 3.12$ and incident angle $\theta_i = \frac{\pi}{4}$.

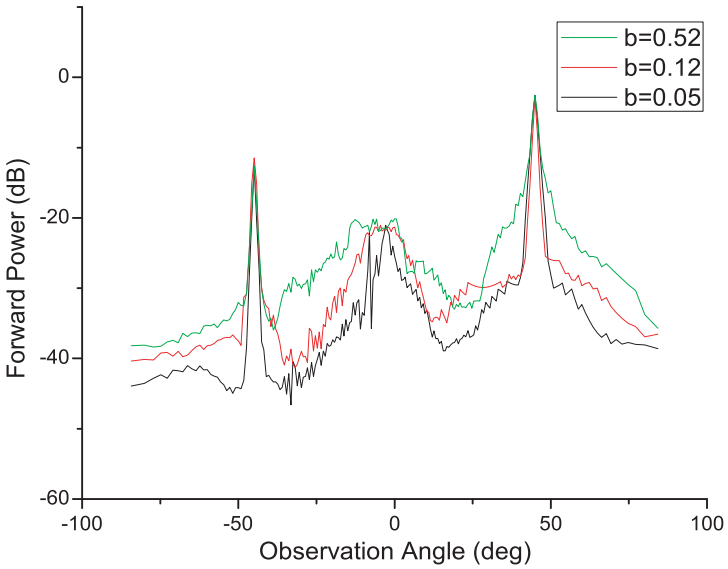

Figure 3. Forward scattered power of a dielectric cylinder for different values of 'b', where $\epsilon_r = 3.12$ and angle of incidence $\theta_i = \frac{\pi}{4}$.

is compensated by the transmitted and diffracted fields to maintain the continuity of the total field across the incident shadow boundary. This diffracted field produces the peaks at this shadow boundary. The power distribution due to field in this region and its association with the width of the cylinder $2b$ is shown in Fig. 3, which shows that as the width of the cylinder is enlarged, the number of guided modes carrying power within the cylinder is increased, so there is an increase in power which comes out from the boundary $x = a$ of the cylinder. As a result, there is an increase in the forward scattering power.

8. CONCLUSION

In this paper, we have concluded that the incident power due to a plane wave on the dielectric cylinder is distributed not only among guided but also among guided and radiation modes. This variation of power among different modes depends upon the width of the cylinder for a constant angle of incidence. If the width of the cylinder is increased, there is an increase of number of modes not only propagating power within the cylinder but also in back and forward scattered power.

ACKNOWLEDGMENT

The author thanks Department of Electronics at the Quaid-i-Azam University, Islamabad for its hospitality during which time this work was commenced.

REFERENCES

1. Froese, C. and J. R. Wait, "Calculated diffraction pattern s of dielectric cylinders at centimetric wavelengths," *Canad. J. Phys.*, Vol. 32, 775–781, 1954.
2. Wait, J. R., *Electromagnetic Radiation by Cylindrical Structures*, Pergamon Press London and New York, 1959.
3. Ohki, M., K. Shimizu, and S. Shogo, "Scattering of Gaussian beam by a dielectric rectangular cylinder," *IEEE Transactions on Electromagnetic Compatibility*, Vol. 42, No. 2, May 2000.
4. Leviatan, Y. and Amir Boag, "Analysis of electromagnetic scattering from dielectric cylinders using a multifilament current model," *IEEE Trans. Antennas and Propagation*, Vol. 35, No. 10, Oct. 1987.
5. Anastassiu, H. T. and J. L. Volakis, "The mode matching technique for electromagnetic scattering by inlets with complex terminations," *Wright Laboratory AARA*, Wright-Patterson AFB, Dayton OH 45 431.
6. Marcuse, D., *Light Transmission Optics; Chapter 8, 9*, Van Nostrand Reinhold Company, New York, NY 10020, 1982.
7. Lewin, L., "On the inadequacy of discrete mode-matching techniques in some waveguide discontinuity problems," *IEEE Transactions on Microwave Theory and Techniques*, Vol. 18, Pages No. 7, Jul. 1970.
8. Widenberg, B., "A general mode-matching technique applied to bandpass radomes," Department of Electroscience Electromagnetic Theory, Lund Institute of Technology Sweden, Aug. 2001.
9. Zhang, K. and D. Li, *Electromagnetic Theory for Microwaves and Optoelectronics*, Springer, New York, 978-3-540-74295-1, 1998.
10. Harrington, R. F., *Field Computation by Moment Method*, IEEE Press, Piscataway, NJ 08855-1331, 1992.
11. Felsen, L. B. and N. Marcuvitz, *Radiation and Scattering of Waves*, IEEE Press, The Institute of Electrical and Electronics Engineers, Inc., New York, 1994.